

Impeding the Medical Protective Clothing Contamination by a Spray Coating of Trifunctional Polymers

Hyeongseop Keum,[†] Dohyeon Kim,[†] Chang-Hee Whang, Aram Kang, Seojung Lee, Woonsung Na, and Sangyong Jon^{*}



Cite This: *ACS Omega* 2022, 7, 10526–10538



Read Online

ACCESS |



Metrics & More

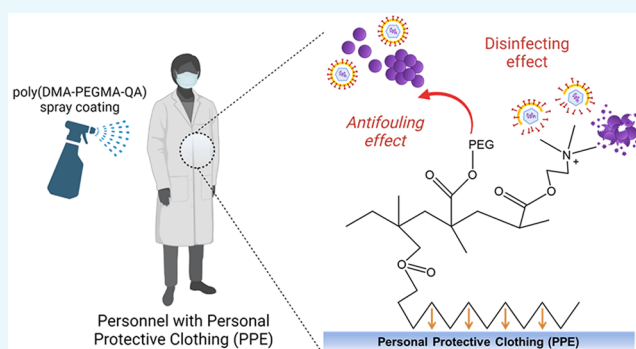


Article Recommendations



Supporting Information

ABSTRACT: The risk of fomite-mediated transmission in the clinic is substantially increasing amid the recent COVID-19 pandemic as personal protective equipment (PPE) of hospital workers is easily contaminated by direct contact with infected patients. In this context, it is crucial to devise a means to reduce such transmission. Herein, we report an antimicrobial, antiviral, and antibiofouling trifunctional polymer that can be easily coated onto the surface of medical protective clothing to effectively prevent pathogen contamination on the PPE. The coating layer is formed on the surfaces of PPE by the simple spray coating of an aqueous solution of the trifunctional polymer, poly(dodecyl methacrylate (DMA)–poly(ethylene glycol) methacrylate (PEGMA)–quaternary ammonium (QA)). To establish an optimal ratio of antifouling and antimicrobial functional groups, we performed antifouling, antibacterial, and antiviral tests using four different ratios of the polymers. Antifouling and bactericidal results were assessed using *Staphylococcus aureus*, a typical pathogenic bacterium that induces an upper respiratory infection. Regardless of the molar ratio, polymer-coated PPE surfaces showed considerable antiadhesion (~65–75%) and antibacterial (~75–87%) efficacies soon after being in contact with pathogens and maintained their capability for at least 24 h, which is sufficient for disposable PPEs. Further antiviral tests using coronaviruses showed favorable results with PPE coated at two specific ratios (3.5:6:0.5 and 3.5:5.5:1) of poly(DMA-PEGMA-QA). Moreover, biocompatibility assessments using the two most effective polymer ratios showed no recognizable local or systemic inflammatory responses in mice, suggesting the potential of this polymer for immediate use in the field.



INTRODUCTION

Pathogens, including severe acute respiratory syndrome coronavirus 2 (SARS-CoV-2), the cause of the COVID-19 pandemic, can be readily transmitted via various routes, including contact, airborne, droplet, fomite, and animal-to-human transmissions. Of these, fomite-mediated transmission is drawing increasing attention because ongoing shortages of personal protective equipment (PPE) require repeated use of contaminated disposable PPEs in the field.¹ Furthermore, various common objects surface-contaminated with respiratory droplets secreted by SARS-CoV-2-infected individuals create fomites with viable pathogens living up to 28 days under ambient environments.^{2–4} Therefore, it is crucial to find ways to control pathogenic contamination on the surface of various PPEs not only in the clinic but also in everyday life around asymptomatic individuals. The primary aim of this study was to develop a disinfecting coating material that is capable of maintaining a PPE surface that is free from fouling with viruses or bacteria for a long duration without safety issues.

Considerable efforts have been made to modify substrates so as to endow them with antibiofouling functionalities. Hydro-

philic polymers such as poly(ethylene glycol) (PEG) and zwitterions are commonly used to weaken the interactions between coated surfaces and potential foulants.^{5–7} Although these polymer brushes hindered the bacterial adhesion and the formation of biofilm, the antifouling property alone without a direct bactericidal property could not eliminate the pathogens that managed to reach the surface through the polymer brushes.^{8,9} In another strategy, surface decorations with antimicrobial peptides, silver- or gold-based nanomaterials, and polycationic compounds have been used to achieve contact-killing of pathogens.^{10–15} However, these approaches for functionalizing the surfaces of fomites require a multistep fabrication process involving hazardous chemical solvents and show antimicrobial potency that is limited to only certain

Received: January 4, 2022

Accepted: March 4, 2022

Published: March 15, 2022



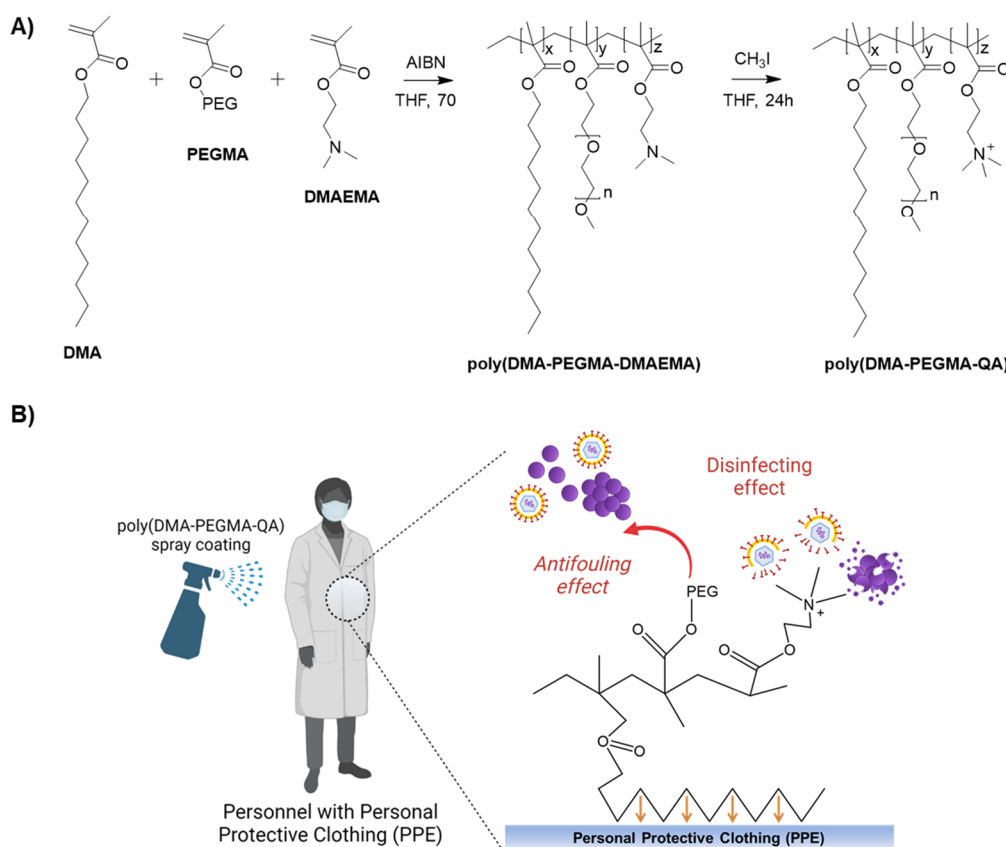


Figure 1. (A) Schematic illustration of the chemical synthesis of poly(DMA-PEGMA-QA) and (B) spray coating of a thin poly(DMA-PEGMA-QA) antibacterial/antiviral coating layer on PPE surfaces.

pathogens; even if it was assumed that these solvents cleared all regulatory processes, these limitations would hamper practical use in the field.^{16–19} Thus, it is vastly more desirable to design a practical, ready-to-use coating material that shows both antibiofouling and antimicrobial efficacy against a broad spectrum of infectious pathogens.

We recently demonstrated that poly(DMA-PEGMA-AA), an amphiphilic polymer with excellent antibiofouling properties composed of dodecyl methacrylate (DMA), poly(ethylene glycol) methacrylate (PEGMA), and acrylic acid (AA), is capable of coating hydrophobic substrates via a one-step immersion process and inhibits the formation of biofilms on the surfaces of urinary catheters.²⁰ The hydrophobic DMA unit in the polymer binds to the hydrophobic surface through multiple van der Waals interactions and functions as an “anchor”, whereas the hydrophilic PEG and AA moieties exert antibiofouling actions.

Traditional antimicrobial agents derived from low molecular weight compounds are prone to resistance, and environmental and health concerns arise after their use due to the diffusion of biocidal agents.^{21,22} Antimicrobial polymeric substances have been proposed as alternatives to address such issues. Among many suggested candidates, antimicrobial polymers involving quaternary ammonium (QA) compounds (e.g., hydrophilic polymers, comb-like polymer brushes, dendritic polymers, etc.)^{23–26} are most commonly used, given the ability of this QA moiety to disrupt the cell membranes of bacteria and viruses with substantially less residual toxicity.^{27–29}

In the current study, we endowed the aforementioned antifouling polymer with antimicrobial and antiviral properties

by replacing the AA monomer with a QA moiety and synthesized poly(DMA-PEGMA-QA) to confer dual antifouling and antimicrobial/antiviral functionalities. An additional finding of note compared to our previous antifouling polymer is that we have tested and confirmed the postmodification of the naïve surfaces of medical protective clothing by a facile spray coating method, which warrants the practicality for use in the field. The following evaluations of the antifouling, antibacterial, and antiviral effects of protective coatings of poly(DMA-PEGMA-QA) were shown to effectively reduce the viability of inbound pathogens. We further conducted biocompatibility tests of polymer-coated PPE fabric *in vitro* by performing cell viability assays and *in vivo* using a skin irritation test.

RESULTS AND DISCUSSION

Formation and Characterization of the Poly(DMA-PEGMA-QA)-Coated PPE Substrate. The antibiofouling and antimicrobial polymer, poly(DMA-PEGMA-QA), was synthesized from the corresponding monomers using a two-step process consisting of radical polymerization and methylation (Figure 1). In the first step, poly(DMA-PEGMA-DMAEMA) was synthesized through radical polymerization of lauryl methacrylate (DMA), poly(ethylene glycol) methacrylate (PEGMA), and 2-dimethylaminoethyl methacrylate (DMAEMA) at four different molar feed ratios of each monomer (3.5:6:0.5, 3.5:5.5:1, 3.5:5:1.5, and 3.5:4.5:2) (Figure S1). In the second step, the tertiary amine group of DMAEMA in each polymer was converted to QA by reacting it with excess iodomethane, yielding four poly(DMA-PEGMA-

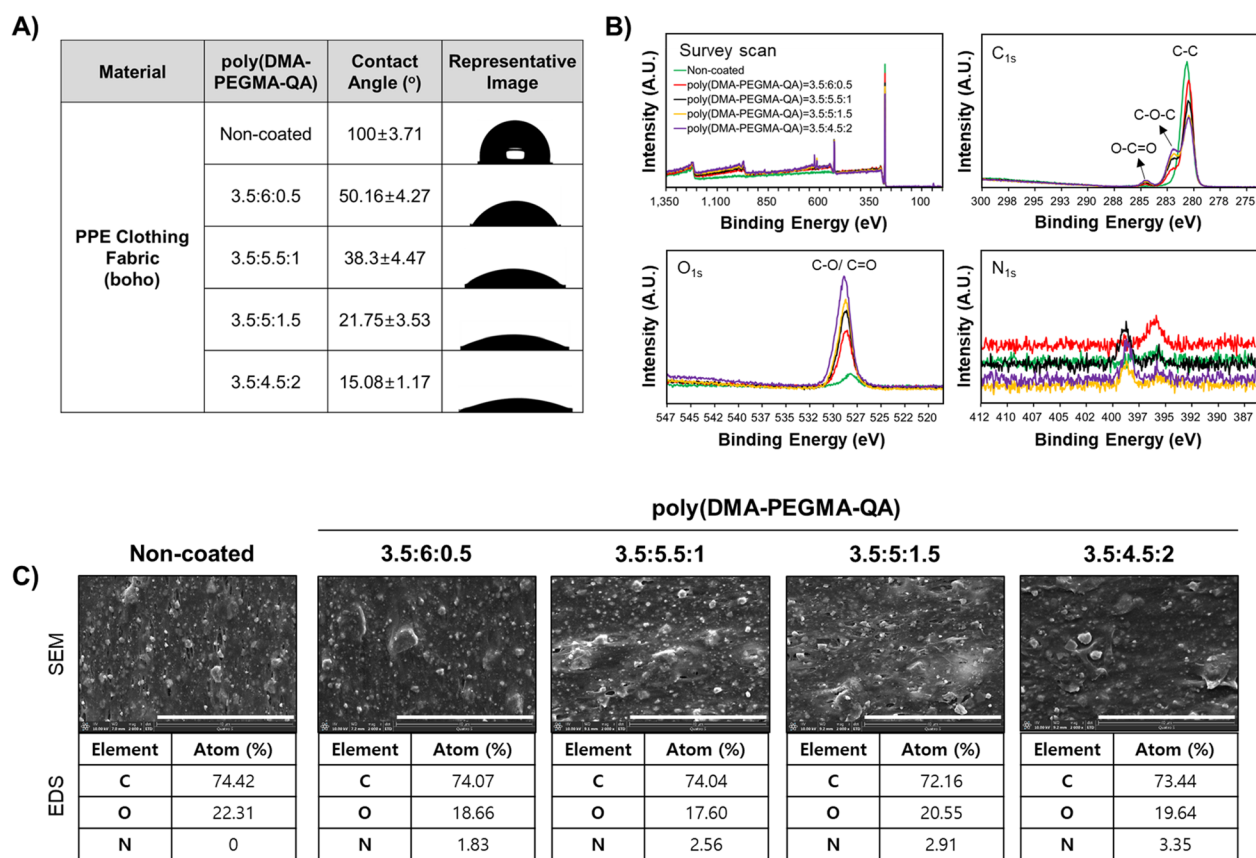


Figure 2. Characterization of poly(DMA-PEGMA-QA)-coated PPE fabric. (A) Static water contact angles of non-coated PPE and polymer-coated PPE surfaces at four different ratios. A purified water droplet (10 μ L) was pipetted onto each surface, and pictures and angle measurements were obtained immediately using a contact angle analyzer. (B) XPS survey and narrow scan spectra of polymer-coated PPE surfaces. The measurements were conducted 7 days after applying a spray coating of poly(DMA-PEGMA-QA). (C) FE-SEM images and broad EDS analyses of uncoated and polymer-coated surfaces. The measurements were performed 24 h after applying the poly(DMA-PEGMA-QA) coating. Scale bars, 40 μ m.

QA) structures (Figure S2). Because of the presence of highly hydrophilic PEG and QA, the final polymers were fairly soluble in an aqueous solution despite the presence of a long alkyl chain DMA moiety. The rationale for maxing out QA content at 20% is based on the fact that most commercially available quaternary ammonium disinfectant concentrates contain no more than 20% QA, as this is sufficient to kill microbes without causing undesirable collateral damage.

The PPE fabric, boho, made from polyolefin fiber, was used as a model medical protective clothing in tests of whether poly(DMA-PEGMA-QA) can be coated onto a substrate through spray coating. It was anticipated that the dodecyl chain of DMA in the polymer would readily anchor onto the hydrophobic surface of the PPE fabric via hydrophobic or van der Waals interactions, resulting in the formation of a nanoscale coating layer, such as that observed in our previous report on urinary catheter coatings (Figure 1B).²⁰ The multiple copies of PEG chains on poly(DMA-PEGMA-QA)-coated substrates are predicted to exert an antiadhesion effect against incoming airborne pathogens,^{30–32} whereas antimicrobial QA groups are expected to disinfect the pathogens in contact with the polymer-coated surfaces by disrupting the negatively charged cell membranes of bacteria or enveloped viruses, causing cell lysis.^{29,33–35} The polymer-coated layers, which were readily formed by spraying an aqueous solution of the polymer (20 mg/mL in water) onto a PPE fabric, were characterized using various means, including static water

contact angle measurements, X-ray photoelectron spectroscopy (XPS), and energy-dispersive X-ray spectroscopy (EDS). Each of these measurements was performed on air-dried fabric samples 1 week after the polymer coating process. The water contact angle of a non-coated PPE fabric was $100^\circ \pm 3.7^\circ$; this angle was dramatically decreased to $50.2^\circ \pm 4.3^\circ$ for a fabric surface coated with poly(DMA-PEGMA-QA) prepared at a monomer ratio of 3.5:6:0.5, indicating that the hydrophobic fabric surface is converted to a hydrophilic surface after the polymer coating process. The contact angle of polymer-coated fabric surfaces decreased as the percentage of QA in the polymer increased, decreasing to $38.3^\circ \pm 4.5^\circ$, $21.8^\circ \pm 3.5^\circ$, and $15.1^\circ \pm 1.2^\circ$ for monomer ratios of 3.5:5.5:1, 3.5:5:1.5, and 3.5:4.5:2, respectively, indicating the successful formation of a polymer coating layer using a spray-coating method (Figure 2A). XPS scans further revealed substantial alterations in the chemical compositions and concentrations of C, O, and N elements present on the four polymer-coated PPE fabric surfaces compared with that of an uncoated PPE fabric. Notable peak changes were observed in C_{1s} narrow scans with peaks corresponding to C–O–C (282 eV) and O–C=O (284.5 eV) bonds being detected only in the polymer-coated surface and not in the parent polyolefin PPE fabric. C–O–C peaks are originated from acrylate and PEG chain groups, and O–C=O peaks are attributed to acrylate groups within the polymer. A significant surge in the oxygen peak at ~ 528 eV was also characteristic of the polymer-coated surface owing to

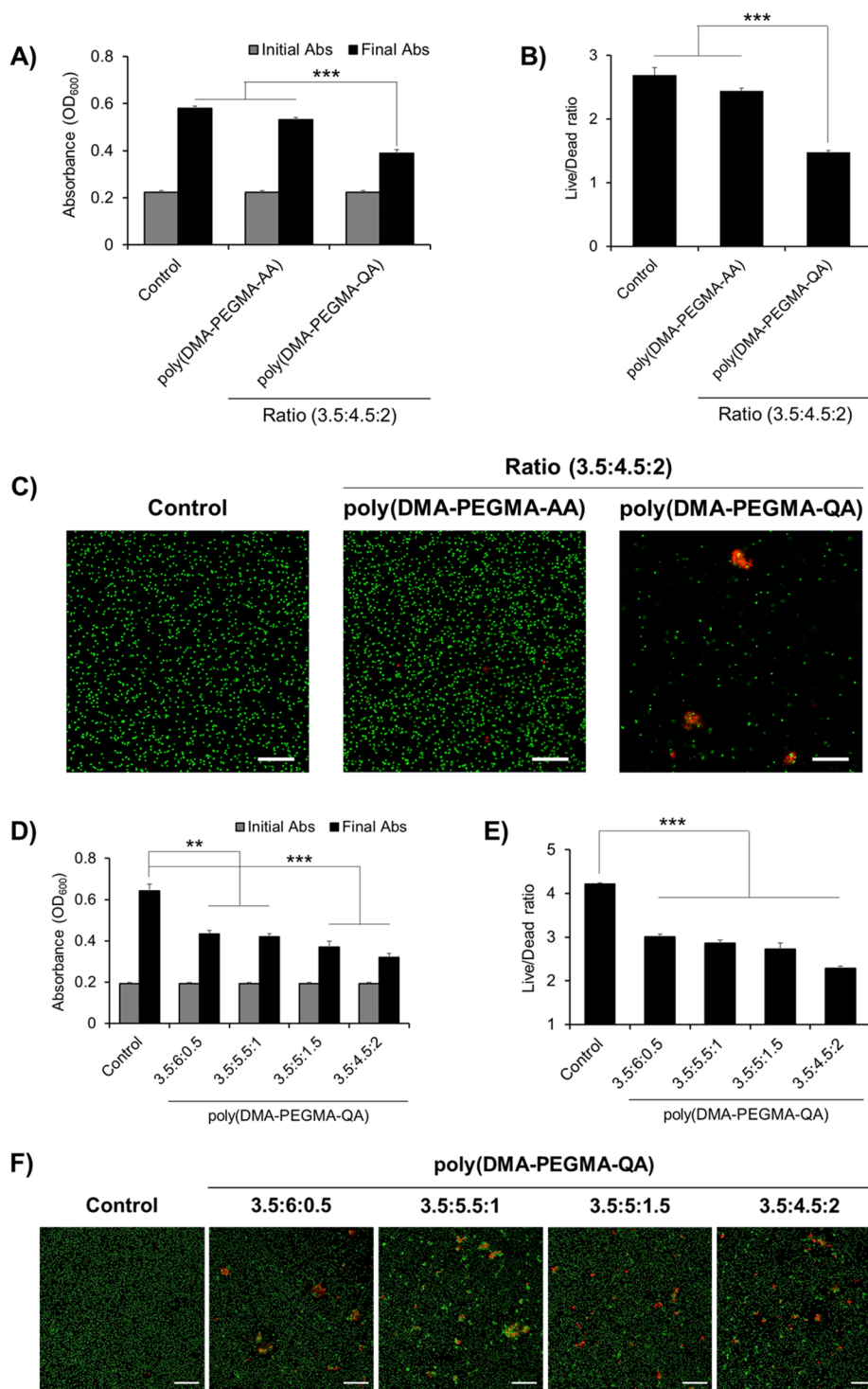


Figure 3. Antibacterial effects of poly(DMA-PEGMA-QA). (A) The antibacterial effect of poly(DMA-PEGMA-QA) was compared with that of our previously reported antifouling polymer without a QA moiety. The respective polymer solution was incubated for 12 h with an *S. aureus* bacterial suspension in PBS buffer at a 1:1 (v/v) ratio to a final concentration of 10 mg/mL, followed by a measurement of optical density. (B, C) After incubation and staining with a L/D bacterial viability kit (live, Ex/Em: 480/500 nm; dead, Ex/Em: 490/635 nm), the viability of the bacterial mixture was determined (B) and representative confocal microscopic images of bacterial solutions were acquired (C). Scale bars, 20 μm. (D) The growth of *S. aureus* culture in LB medium mixed with antimicrobial polymer was measured. The bacterial suspension in LB (OD₆₀₀ ≈ 0.2) was incubated for 24 h in a 37 °C shaking incubator at a 1:1 (v/v) ratio with poly(DMA-PEGMA-QA) solution at a final concentration of 10 mg/mL. (E) After the 24 h incubation, the viability of the bacterial samples was quantified using a L/D bacterial viability kit. (F) Representative confocal images of bacterial suspensions after incubation with the indicated ratios of poly(DMA-PEGMA-QA). Scale bars, 20 μm. Data are presented as means ± SEM (****p* < 0.001, ***p* < 0.01, **p* < 0.05; one-way ANOVA followed by Tukey's post hoc test).

the presence of oxygen within acrylate and PEG chain groups, in keeping with the barely existent oxygen in the parent PPE

fabric. Lastly, only polymer-coated surfaces displayed nitrogen peaks owing to the presence of the QA moiety (Figure 2B).

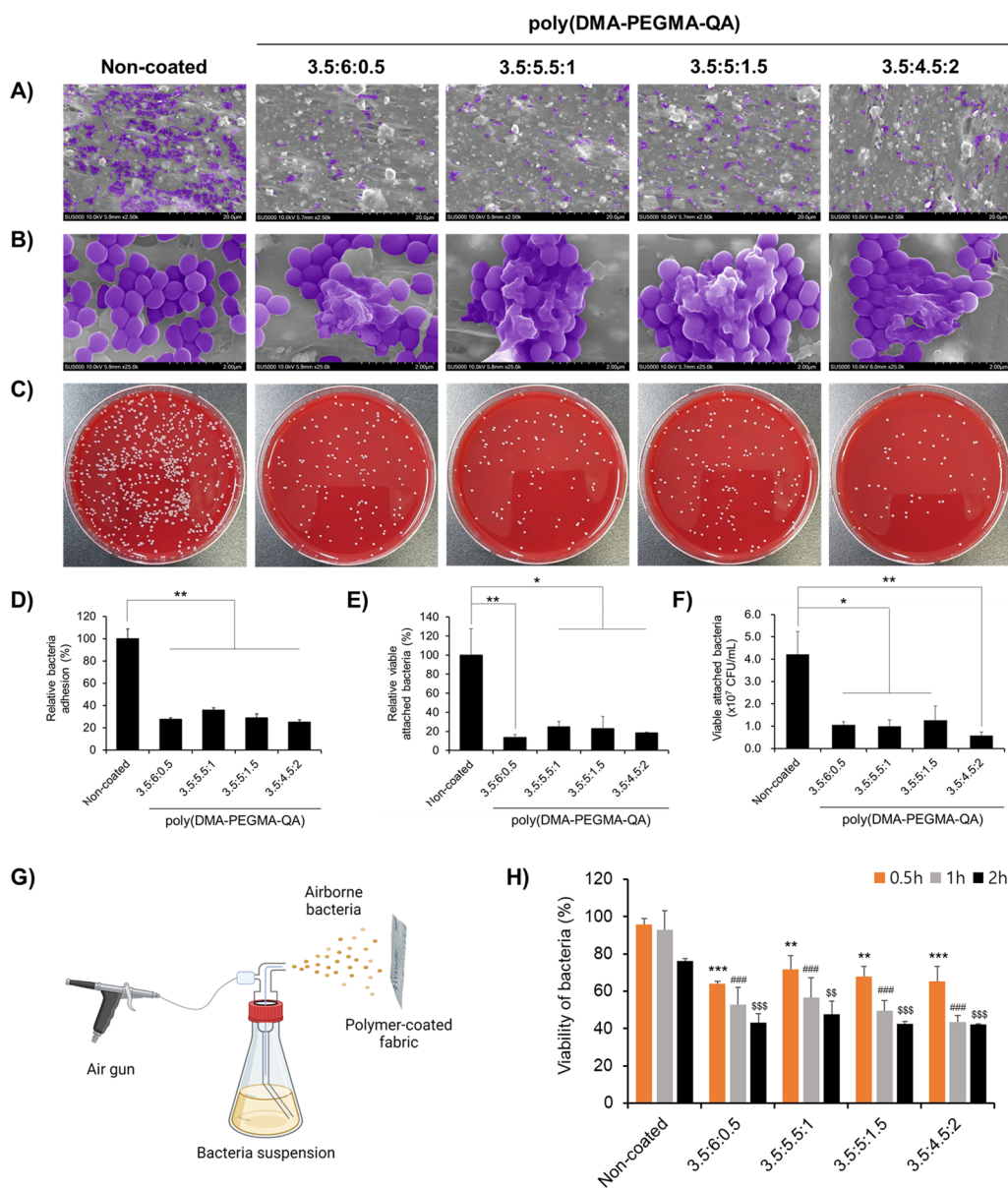


Figure 4. Antifouling and antibacterial effects of a poly(DMA-PEGMA-QA)-coated PPE surface. (A) The antifouling efficacy of poly(DMA-PEGMA-QA)-coated PPE was validated by FE-SEM imaging. *S. aureus* in LB media (3.0×10^6 CFU/mL) was incubated for 24 h in a 37 °C incubator. The incubated PPE was washed with PBS buffer to remove unattached bacteria, followed by dehydration and fixation for FE-SEM imaging. Scale bars, 20 μm . (B) Representative FE-SEM images of membrane-disrupted *S. aureus* resulting from the antibacterial effect of the QA moiety in poly(DMA-PEGMA-QA). Scale bars, 2 μm . (C) The antibacterial effects of PPE spray-coated with 20 mg/mL poly(DMA-PEGMA-QA) at various molar ratios. Polymer-coated PPE was incubated with *S. aureus* in LB media (3.0×10^6 CFU/mL) for 24 h in a 37 °C incubator. Bacteria on the PPE surface were detached by mild vortexing and sonication, followed by spreading (100 μL) on blood agar plates at appropriate dilutions for quantification of viable bacteria. (D) The antiadhesion effect of the poly(DMA-PEGMA-QA)-coated PPE surface was quantified using crystal violet staining. The color intensities of surface-remaining bacteria were measured at 590 nm. (E) Viable bacteria on polymer-coated PPE after a 24 h incubation were quantified using a WST-8 viability assay. The color intensities of surface-remaining viable bacteria were measured at 450 nm. (F) Viable bacteria on polymer-coated PPE after incubation were assessed on the basis of colony-forming units (CFUs). (G) Experimental scheme of the antimicrobial test in an airborne condition. (H) The PPE fabrics applied with airborne bacteria were incubated for 0.5, 1, and 2 h at ambient temperature, respectively. The incubated bacteria were detached by gentle vortexing and sonication followed by measurements of the viability of collected bacteria using the L/D bacterial viability kit. All data are represented as mean \pm standard deviation. A two-way ANOVA with a Bonferroni posthoc test was performed. Compared with non-coated PPE fabrics at 30 min, * $p < 0.05$, ** $p < 0.01$, and *** $p < 0.001$; at 1 h, # $p < 0.05$, ## $p < 0.01$, and ### $p < 0.001$; at 2 h, § $p < 0.05$, §§ $p < 0.01$, and §§§ $p < 0.001$.

We noticed slight nitrogen peak shifting for the 3.5:6:0.5 ratio, but small changes in the X-ray radiation power and chamber temperature can cause minimal peak shifting in the margin of error; thus, it was not taken into account.^{36,37} Matrix-assisted laser desorption ionization time-of-flight (MALDI-TOF) measurements of polymers showed (Figure S3) the peaks at

700–1200, 1200–1700, 1700–2200, and 2200–2700 (m/z) regions. The most abundant polymer mass ranged from 900 to 1200, and additional mass peaks were observed in 450 to 500 increments. Since poly(DMA-PEGMA-QA) is a random copolymer, we expect such mass increment values to correspond to mono-PEGMA, di-DMA, tri-QA, mono-DMA,

and di-QA. Besides, due to PEG in PEGMA, constant spacing between each peak with a m/z value of around 44 was observed (Figure S3).

Scanning electron microscopy (SEM) and the corresponding EDS measurements showed increasing concentrations of nitrogen on polymer-coated surfaces with an increase in the ratio of QA in the polymer (Figure 2C). The surface roughness of each polymer-coated fabric surface, analyzed by atomic force scanning microscopy (AFM), remained low at different monomer molar ratios: 95.4 nm for 3.5:6:0.5, 103 nm for 3.5:5.5:1, 90.7 nm for 3.5:5:1.5, and 57.4 nm for 3.5:4.5:2, suggesting that the wear rate of the polymer layer due to abrasion and friction should remain low (Figure S4).³⁸ Furthermore, to demonstrate the durability of the polymer coating, we analyzed the water contact angle of polymer-coated (3.5:4.5:2 ratio as a representative) PPE fabrics for 7 days consecutively. Initially, consistent with our prior contact angle measurements for coating evaluation, we observed a substantial decrease of the water contact angle to $\sim 28.7^\circ \pm 2.2^\circ$, reassuring the formation of a hydrophilic coating layer. Throughout the daily measurements of the contact angle for 7 days, no notable changes were observed, suggesting that once formed the polymer coating layer is stable for at least 7 days (Figure S5A). Furthermore, the contact angle measurements of polymer-coated PPE kept in a moisturized condition ($\sim 80\%$ humidity) were reliably stable for at least 24 h, reassuring the stability of the formed spray-coated polymer layer in a practical situation where PPE can be easily exposed to a humidified condition (Figure S5B). Collectively, these characterizations indicate that the polymer coating layer is readily formed on a PPE fabric substrate by a simple spraying method. Besides, although currently used PPEs in the field are mostly disposable due to the contamination and related health concerns, our coated polymer layer is stable for at least 7 days, possibly elongating the lifespan of conventional PPEs.

Antibacterial Effects of Poly(DMA-PEGMA-QA) in an Aqueous Solution. Unlike poly(DMA-PEGMA-AA), which has only antibiofouling properties, poly(DMA-PEGMA-QA) is expected to exhibit both antibiofouling and antibacterial properties owing to the presence of QA.²⁰ *S. aureus*, one of the most common bacteria strains that cause respiratory infections,^{39–41} was used to examine antibacterial effects of poly(DMA-PEGMA-QA). Bacteria in phosphate-buffered saline (PBS) at an optical density at 600 nm (OD_{600}) of ~ 0.2 were incubated at a 1:1 v/v ratio with 20 mg/mL poly(DMA-PEGMA-AA) or poly(DMA-PEGMA-QA) at a monomer ratio of 3.5:4.5:2 (final polymer concentration: 10 mg/mL). Whereas poly(DMA-PEGMA-AA) showed negligible antibacterial effects, poly(DMA-PEGMA-QA) showed substantial bactericidal efficacy, as evidenced by a decrease in OD_{600} to 0.38 versus 0.58 in the controls; by comparison, the OD_{600} for poly(DMA-PEGMA-AA) was 0.53 (Figure 3A). Live/Dead (L/D) viability assays confirmed the notable antibacterial effect of poly(DMA-PEGMA-QA), which exhibited an L/D ratio of 1.47, a value much lower than that for untreated controls (2.69) and poly(DMA-PEGMA-AA) (2.44) (Figure 3B). Fluorescence imaging using SYTO 9, which is detected as green fluorescence in live bacteria, and propidium iodide (PI), which fluoresces red in apoptotic bacteria, further confirmed that poly(DMA-PEGMA-QA) treatment led to large numbers of dead bacterial aggregates (Figure 3C). Next, we assessed the antibacterial effects of poly(DMA-PEGMA-QA) under harsher conditions. Specifically, four poly(DMA-

PEGMA-QA) formulations prepared from four different molar ratios of each monomer were incubated with suspensions of *S. aureus* bacteria in Luria broth (LB) media ($OD_{600} \approx 0.2$) at a final concentration of 10 mg polymer/mL for 24 h. All polymers effectively suppressed bacterial growth even in LB media conditions (Figure 3D). As expected, an increase in the QA ratio in the polymer resulted in greater bactericidal efficacy with ratios of 3.5:6:0.5, 3.5:5.5:1, 3.5:5:1.5, and 3.5:4.5:2 producing OD_{600} values of 0.43, 0.42, 0.37, and 0.32, respectively, compared with 0.64 for the controls. A similar trend was observed for L/D assays (Figure 3E) and fluorescence imaging of live and dead cells (Figure 3F). Collectively, these results clearly indicate that poly(DMA-PEGMA-QA), unlike poly(DMA-PEGMA-AA), exerts a considerable bactericidal effect in a manner that is proportional to the content of the permanently positively charged QA moiety in the polymer.

Antibiofouling and Antibacterial Effects of Poly(DMA-PEGMA-QA)-Coated PPE Fabric Surfaces. Having confirmed the successful coating of poly(DMA-PEGMA-QA) on a PPE fabric surface and the considerable antibacterial effect of poly(DMA-PEGMA-QA) in solution, we next examined the antibiofouling and bactericidal effects of the polymer coating on a commercially available PPE using *S. aureus*. We first incubated a solution of *S. aureus* (3.0×10^6 CFU/mL in LB) on polymer-coated PPE surfaces for 24 h at 37°C and then tested whether the polymer-coating layer could block non-specific adsorption of bacteria on the corresponding surface. SEM images revealed substantial amounts of individual and aggregated bacteria on a bare PPE fabric surface, whereas the number of bacteria was remarkably reduced on polymer-coated surfaces regardless of monomer ratio (Figure 4A). In higher magnification (25 000 \times) representative SEM images, we were also able to observe that bacteria incubated on a bare PPE surface showed an intact phenotype, whereas bacterial morphology was distorted on all surfaces coated with poly(DMA-PEGMA-QA) regardless of the ratio owing to cellular membrane disruption by the presence of QA (Figure 4B). This observation suggests that poly(DMA-PEGMA-QA) may also be effective against drug-resistant microbes, pathogens rapidly becoming a problem in hospitals.⁴² Representative images of incubated agar plates after spreading of surface-detached bacteria showed an obvious reduction in bacterial viability (Figure 4C). We next performed quantitative analyses of the antibiofouling and antibacterial potency of PPE surfaces coated with poly(DMA-PEGMA-QA). Crystal violet (CV) assays confirmed a reduction in the adhesion of *S. aureus* onto polymer-coated PPE fabric surfaces that ranged from $\sim 65\%$ to 75% depending on the content of the QA moiety in each polymer (Figure 4D). This reduced bacterial adhesion may be attributable to the presence of multiple PEG groups on the polymer-coated surfaces.^{43,44} Next, the viability of bacteria remaining on the surfaces was quantified using a commercial WST-8 assay and an analysis of bacteria colony-forming units (CFUs). WST-8 assays revealed significant reductions ($\sim 75\text{--}87\%$) in live bacteria on all poly(DMA-PEGMA-QA)-coated substrates regardless of monomer ratio (Figure 4E). For bacterial CFU assays, *S. aureus* remaining on surfaces after incubation were detached by gentle vortexing and sonication, and the detached bacterial solution was spread on blood agar plates at different dilution factors. CFU counts performed at a 10 000 \times dilution revealed that poly(DMA-PEGMA-QA)-coated PPE was consistently effective in reducing the viability

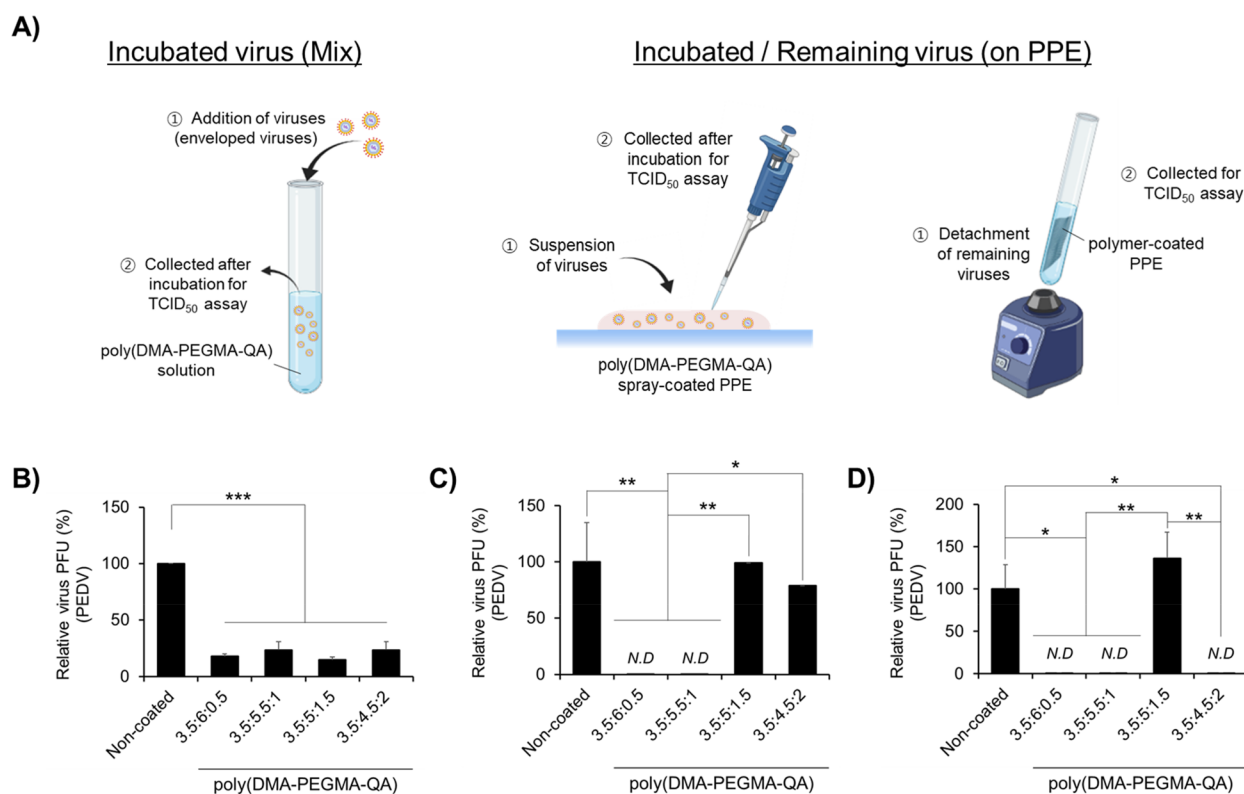


Figure 5. Antiviral effect of poly(DMA-PEGMA-QA)-coated PPE surface against coronavirus. (A) Experimental schemes of the conducted antiviral tests. (B) The virucidal effect of poly(DMA-PEGMA-QA) against coronavirus was measured by mixing a 20 mg/mL solution of poly(DMA-PEGMA-QA) and PEDV suspension at a 1:1 (v/v) ratio for 1 h in a 4 °C incubator. After incubation, viable coronaviruses were assessed by performing TCID₅₀ assays. (C) Antiviral effect of PPE surfaces spray-coated with 20 mg/mL poly(DMA-PEGMA-QA) at various molar ratios. Polymer-coated PPEs were incubated with coronavirus in culture media (DMEM supplemented with 0.3% tryptone phosphate broth, 0.02% yeast extract, and 2 μg of trypsin) for 1 h in a 4 °C incubator. After incubation, the virus suspension was collected for TCID₅₀ assays. (D) Surface-remaining viruses on the PPE substrate were detached by vortexing, and TCID₅₀ assays were performed. N.D, nondetected. Data are presented as means ± SEM (***p* < 0.001, ***p* < 0.01, **p* < 0.05; one-way ANOVA followed by Tukey's post hoc test).

of contacting *S. aureus* by ~70–86% (Figure 4F). On the other hand, a poly(DMA-PEGMA-AA) coating without the quaternary ammonium group did not exert an efficient antibacterial effect as much, probably due to the absence of a direct bactericidal QA functional moiety, suggesting the necessity of antibacterial efficacy on top of the antifouling property (Figure S6). Further long-term antibacterial test of polymer-coated (3.5:4.5:2 ratio as a representative) PPE fabrics showed that the functionality of the poly(DMA-PEGMA-QA) layer was stable for at least 7 days supporting the durability of the coating layer (Figure S7).

Furthermore, we also experimented the antimicrobial function of poly(DMA-PEGMA-QA)-coated PPE fabrics against airborne bacteria to simulate the natural propagation of aerosol pathogens. Each poly(DMA-PEGMA-QA)-coated PPE fabric was sprayed with a suspension of *S. aureus* (5.0×10^8 CFU/mL in 0.85% NaCl) and incubated for 0.5, 1, and 2 h at ambient temperature (Figure 4G). After the incubation, the bacteria on each PPE fabric were detached via vortexing and the viability of the bacteria was assessed using the L/D bacterial viability kit. Regardless of the ratio, the viability of airborne bacteria sprayed and incubated on poly(DMA-PEGMA-QA)-coated PPE fabrics rapidly reduced starting at an early time point of 0.5 h. Within 0.5 h of exposure to the poly(DMA-PEGMA-QA) layer, the viability of airborne bacteria was decreased by ~29–35% compared to that of the non-coated fabric. As we analyzed for longer periods, we

witnessed a further reduction in airborne bacteria in contact with the poly(DMA-PEGMA-QA) layer, and by the time of the 2 h incubation, the viability dropped to ~42–47% compared to the control for all ratios (Figure 4H). Collectively, separate from the monomer ratios, PPE fabrics spray-coated with poly(DMA-PEGMA-QA) are capable of effectively killing pathogens within a short period (<0.5 h) in a bacteria airborne condition mimicking the actual circumstances. Despite our effort to find the optimized monomer ratios of the polymer, the combined antifouling and antibacterial results between polymers of varying monomer ratios were marginal. This was probably because, unlike the previous surface graftable polymer with 35–45% quaternization,^{42,45} we have limited the biocidal QA content of our polymer to 20% in an effort to minimize the biocompatibility concern, and content changes of PEG and QA were rather not drastic among the groups. For future reference, analysis using a polymer with higher QA composition may exhibit improved results with tendencies. However, to use such polymers in practice, thorough biocompatibility tests will be required to pass safety regulations.

Antiviral Effects of Poly(DMA-PEGMA-QA) and Polymer-Coated PPE Fabric Surfaces. We next investigated the antiviral effects of poly(DMA-PEGMA-QA) and polymer-coated PPE surfaces against porcine epidemic diarrhea virus DR13 (PEDV), a coronavirus that bears a structural resemblance to the prevailing SARS-CoV-2 (Figure 5A).^{46–48}

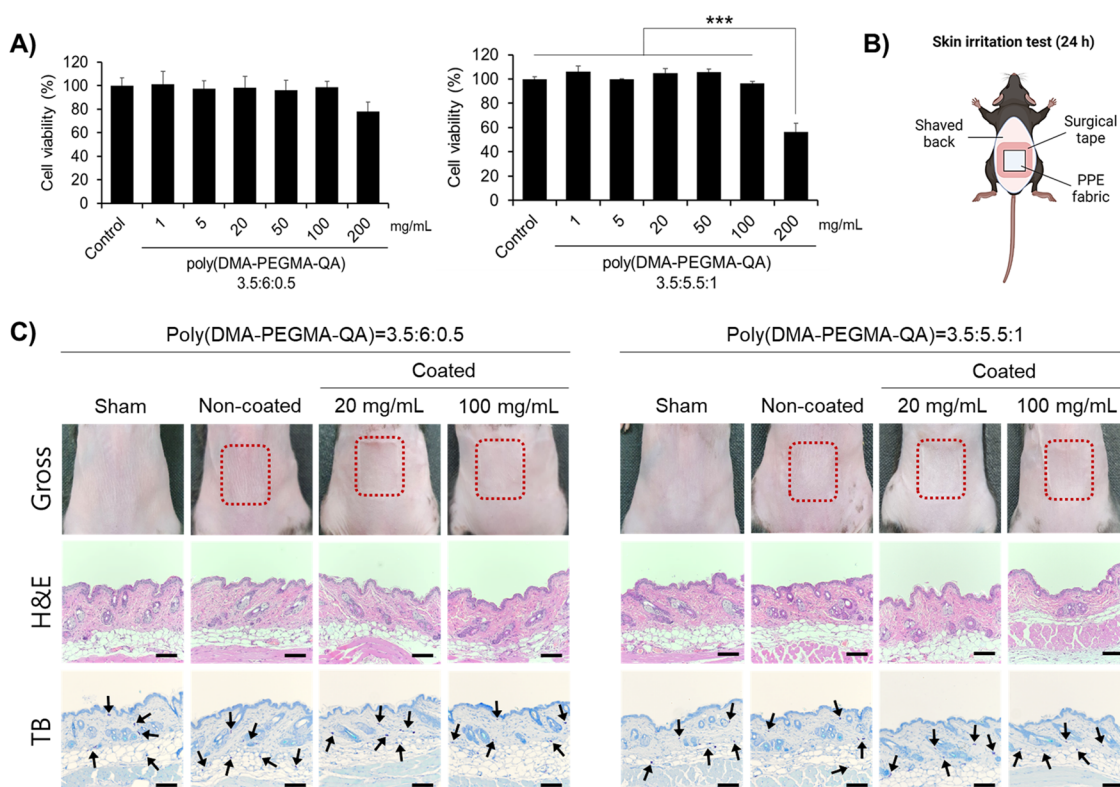


Figure 6. Biocompatibility assessment of poly(DMA-PEGMA-QA)-coated PPE. (A) The viability of NIH3T3 cells on polymer-coated cell culture plates. Cell viability was measured using WST-8 assays after a 24 h incubation at 37 °C in a humidified 5% CO₂ chamber. (B) Schematic illustration of the skin irritation test. (C) Representative images of gross and H&E and toluidine blue (TB) staining of skin in contact with PPE coated with the working concentration (20 mg/mL) and the highest polymer concentration without *in vitro* toxicity (100 mg/mL) of poly(DMA-PEGMA-QA). Polymer-coated PPE was attached to the shaved back of C57BL/6 mice for 24 h and analyzed for inflammatory responses on the basis of objective Draize scoring (data not shown) and histological images. The arrows indicate mast cells in the skin. Scale bars, 200 μm. Data are presented as means ± SEM (***p* < 0.001, ***p* < 0.01, **p* < 0.05; one-way ANOVA followed by Tukey's post hoc test).

Antiviral effects of poly(DMA-PEGMA-QA) *per se* in aqueous solution were tested by incubating PEDV with poly(DMA-PEGMA-QA) at a 1:1 (v/v) ratio for 1 h at 4 °C. Subsequent assays of the 50% tissue culture infectious dose (TCID₅₀) showed that the polymers substantially reduced (by ~76–86%) the viability of coronavirus in a manner that depended on the ratio of each monomer (Figure 5B), indicative of their antiviral activity. Next, we assessed the antiviral effects of poly(DMA-PEGMA-QA)-coated PPE surfaces. PEDVs were suspended on each polymer-coated PPE for 1 h at 4 °C, and their antiviral activity was assessed by measuring TCID₅₀ values of viable viruses remaining both in solution and on the coated surfaces (Figure 5A). Viruses remaining on the surfaces were detached by gentle vortexing. Interestingly, poly(DMA-PEGMA-QA)-coated PPE surfaces showed a trend in antiviral activity different from that obtained using an aqueous solution of the polymers, which showed considerable antiviral activity regardless of monomer ratio. Specifically, whereas PPE surfaces coated with polymers with monomer ratios of 3.5:6:0.5 and 3.5:5:5:1 exerted high antiviral efficacy, polymer-coated surfaces coated with polymers with monomer ratios of 3.5:5:1.5 and 3.5:4.5:2 were ineffective in reducing virus viability compared with the uncoated bare PPE surface (Figure 5C,D). Although this unexpected result is difficult to interpret, it is clear that poly(DMA-PEGMA-QA) containing a relatively lower QA molar ratio (0.5 or 1.0) and PPE surfaces coated with it exert strong antiviral activity against the coronavirus, PEDV. However, although PEDV and SARS-

CoV-2 share similar physical structures, further in-depth studies are necessary to emphasize the effectiveness of our antimicrobial coating against prevailing SARS-CoV-2 and its mutant derivatives.

Biocompatibility of Poly(DMA-PEGMA-QA)-Coated PPE Substrates. The biocompatibility of poly(DMA-PEGMA-QA) with monomer ratios of 3.5:6:0.5 and 3.5:5:5:1, which exerted potent antibacterial and antiviral activity, was evaluated *in vitro* and *in vivo*. For cell viability assays, each polymer was coated onto a conventional polystyrene-based cell culture plate under aqueous conditions,⁴⁹ and fibroblasts (NIH3T3 cells) were cultured on coated plates for 24 h at 37 °C. Unlike their demonstrated toxicity against bacteria and coronavirus at a working concentration (20 mg/mL), neither polymer-coated surfaces affected the viability of fibroblasts up to a 5-fold higher polymer concentration, 100 mg/mL (Figure 6A), suggesting that these polymers are selectively biocompatible with mammalian cells compared to bacteria and viruses. Further *in vivo* biocompatibility tests were performed using each polymer-coated PPE fabric substrate, as illustrated in Figure 6B. Symptoms of skin irritation and corrosion were assessed after attaching each polymer-coated PPE onto the shaved back of a mouse for 24 h, a paradigm chosen to simulate real-world conditions in which medical personnel wear protective clothing for a longer period without removing it for disposal. This is a far more rigorous condition than the standard skin irritation assessment protocol (chemical–skin interaction time ≤ 4 h)

described in the Globally Harmonized System (GHS) for classification and labeling of chemicals and Organization for Economic Co-operation and Development (OECD) guidelines. The characteristic erythematous rash and desquamation of skin under the condition of inflammation were not observed.⁵⁰ Further histological evaluation using hematoxylin and eosin (H&E) and toluidine blue (TB) staining revealed that local skin tissues applied with PPE fabrics coated with either polymer ratios at 20 and 100 mg/mL produced few clinical symptoms of skin irritation, as determined by infiltration of inflammatory and mast cells and Draize scoring (data not shown) (Figures 6C and S8). In addition, splenomegaly was not observed, indicating that there was no systemic inflammatory immune cell accumulation (Figure S9). It has been well reported that splenomegaly is related to various infectious and systemic inflammatory diseases. The total number of splenocytes and spleen mass are increased in the systemic inflammation, as the spleen is a secondary lymphoid organ.⁵¹ In particular, spleen enlargement could provide appropriate prognosis information for systemic mastocytosis in which mast cells accumulate in the skin from the inflammatory response.⁵² Collectively, our results indicate that poly(DMA-PEGMA-QA)-coated PPE surfaces can be considered biocompatible and safe for use.

CONCLUSIONS

In this study, we demonstrated that the trifunctional polymer, poly(DMA-PEGMA-QA), can form a durable coating layer on polyolefin-based PPE fabrics using a simple one-step spraying process and that the resulting polymer-coated surfaces exert strong antibacterial and antiviral effects. It should be noted that, owing to the hydrophilic components of poly(DMA-PEGMA-QA), this type of polymer is fairly soluble in aqueous solution, circumventing possible biocompatibility issues of other antimicrobial polymers that involve the use of alcohol or hazardous chemical solvents. We also demonstrated the importance of the quaternary ammonium (QA) moiety and further established optimal molar ratios in poly(DMA-PEGMA-QA) for antibacterial and antiviral effects. Finally, biocompatibility tests showed that poly(DMA-PEGMA-QA)-coated surfaces do not induce any noticeable toxicities against fibroblasts *in vitro* or skin *in vivo*, suggesting the possibility of immediate use in the field. Taken together, our findings suggest that the antifouling, antimicrobial, and antiviral trifunctional polymer demonstrated herein can be used to minimize fomite-mediated transmission of various pathogens, including SARS-CoV-2, by a simple spray coating of medical or other protective clothing surfaces. This easy-to-use, multifunctional polymer coating holds significant promise in stopping fomite transmission of fatal pathogens in the prevailing pandemic environment.

MATERIALS AND METHODS

Polymer Synthesis. Poly(DMA-PEGMA-QA) was synthesized as depicted in Figure 1A. The monomers, dodecyl methacrylate (DMA) (Sigma-Aldrich, St. Louis, USA), poly(ethylene glycol) methyl ether methacrylate (PEGMA, $M_n \sim 500$) (Sigma-Aldrich), and 2-dimethylaminoethyl methacrylate (DMAEMA) (Sigma-Aldrich) at molar ratios of 3.5:4.5:2, 3.5:5:1.5, 3.5:5.5:1, and 3.5:6:0.5 were dissolved in anhydrous tetrahydrofuran (THF; 3 mL per 2 g of monomers), and the mixtures were purged with nitrogen for 10 min. Reversible

addition–fragmentation chain-transfer (RAFT) polymerization was carried out using 2,2'-azobis(2-methylpropionitrile) (AIBN) (Sigma-Aldrich) as an initiator (2% of total mmol) and 2-cyano-2-propyl benzodithioate as a chain-transfer agent (3.5% of total mmol) at 70 °C for 16 h under nitrogen. After the reaction, polymerization was quenched by exposure to air, and the reaction mixtures were purified by dialysis against distilled water for 48 h, followed by lyophilization to obtain the intermediate polymer, poly(DMA-PEGMA-DMAEMA). Finally, dimethylaminoethyl (DMAE) groups in the respective polymers were converted into quaternary ammonium (QA) groups by reacting the polymers with excess methyl iodide in anhydrous THF for 24 h at room temperature. Upon completion of the reaction, THF was removed using a rotary evaporator and the solution was vacuum desiccated for at least 24 h. Synthesis of the final product was confirmed by ¹H NMR spectroscopy using a 400 MHz NMR spectrometer (Bruker 400; Bruker Optics, Billerica, MA, USA).

Preparation of Polymer-Coated PPE Fabrics. Polyolefin-based PPE fabric (boho) was kindly provided by UPC LTD (Chungcheongnam-do, Korea). The PPE fabrics were cut to a uniform size (1.5 × 1.5 cm) and brushed off using an air compressor gun to remove impurities. Each viscous poly(DMA-PEGMA-QA) concentrate was dissolved in distilled water to 20 mg/mL. After the polymer solution was sprayed on the PPE surface using a perfume atomizer, it was dried overnight at room temperature.

Characterization of Polymer-Coated PPE Fabrics. Non-coated PPE surfaces and poly(DMA-PEGMA-QA)-coated PPE surfaces were prepared for static contact angle measurements. A drop of distilled water (10 μL) was pipetted onto each surface, and contact angles were measured immediately in triplicate using a contact angle analyzer (Phoenix 300 Plus; SEO, Kyonggi-do, Korea) and averaged. For long-term contact angle measurements, PPE fabrics coated with poly(DMA-PEGMA-QA) at a monomer ratio of 3.5:4.5:2 for the indicated time (in days) were used for the analysis. Changes in chemical composition after polymer spray coating of PPEs were characterized using X-ray photoelectron spectroscopy (Sigma Probe Multipurpose XPS; K-alpha, Thermo VG Scientific). XPS survey scan spectra (base pressure maintained at 2.0×10^{-9} mb) were obtained using a monochromatic Al K α radiation X-ray source (12 kV, KE = 1486.6 eV) and analyzed over the range of 0–1350 eV. Different elemental narrow scans were subsequently recorded over their corresponding range: C_{1s}, 274–300 eV; O_{1s}, 518–547 eV; N_{1s}, 386–412 eV. The MALDI-TOF mass spectra were measured via an Autoflex MALDI-TOF mass spectrometer (BrukerDaltonics, Billerica, MA, USA) with an Nd:YAG laser of 355 nm, duration pulse of 3 ns, and accelerating voltage of 20 kV. Each polymer solution was mixed with the 2,5-dihydroxybenzoic acid (DHB) matrix in a ratio of 1:2 (v/v) and loaded onto the stainless steel sample plate. All samples were air-dried before MALDI-TOF analysis. The uniformity of coating over the larger area was analyzed by examining the morphology and composition of polymer-coated PPE fabrics on an expanded scale using a field-emission scanning electron microscope (FE-SEM) equipped with energy-dispersive X-ray spectroscopy (EDS) (Magellan 400; FEI, Hillsboro, USA). All samples were coated with platinum (30 s) before FE-SEM analysis.

Antibacterial and Growth Inhibition Effects of Poly(DMA-PEGMA-QA). *S. aureus* (ATCC 25923) was grown in

Luria broth (LB) media (Conda, Madrid, Spain) in a shaking incubator at 37 °C. First, to compare the antibacterial performance of poly(DMA-PEGMA-QA) with our previous antifouling polymer, poly(DMA-PEGMA-AA), we diluted a solution of *S. aureus* in PBS ($OD_{600} \approx 0.2$) and mixed it at a 1:1 (v/v) ratio with each polymer, synthesized at an equal molar feed ratio to a final concentration of 10 mg/mL. After incubation overnight (~12 h) in a shaking incubator at 37 °C, the OD_{600} of the mixture was measured. The viability of bacteria in the mixture was estimated using a Live/Dead bacterial viability kit (L7012; Invitrogen, Carlsbad, CA, USA). Bacteria incubated with the polymer solution were stained with SYTO9 (live, green; Ex/Em: 480/500 nm) and PI (dead, red; Ex/Em: 490/635 nm). The fluorescence intensities of live and dead bacteria were quantified using a microplate reader (Molecular Devices, Sunnyvale, CA, USA). Representative fluorescence images were acquired by pipetting stained bacteria samples into a μ -slide (Ibidi, Gräfelfing, Germany) and analyzed using a confocal laser-scanning microscope (LSM 780; Carl Zeiss, Oberkochen, Germany). In optimization experiments, the bacterial growth-inhibition efficacy of poly(DMA-PEGMA-QA) was assessed at all four molar ratios. *S. aureus* cultures were diluted in LB media ($O.D_{600} \approx 0.2$) and mixed 1:1 (v/v) with poly(DMA-PEGMA-QA) at a concentration of 20 mg/mL. After overnight incubation in a shaking incubator at 37 °C, live and dead bacteria were quantified and assessed using the aforementioned protocols.

Antiadhesion Effect of Poly(DMA-PEGMA-QA)-Coated PPE Fabrics. PPE fabrics spray-coated with different molar ratios were washed with distilled water to remove excess polymer solution. *S. aureus* concentration was diluted to 3.0×10^6 CFU/mL (in LB media), and a 50 μ L aliquot was pipetted onto PPE fabrics. After incubation at 37 °C for 24 h, unattached bacteria were removed by washing twice with 1 \times PBS. Next, prepared PPE clothing fabrics were fixed with 4% formaldehyde (w/v) and dehydrated by successively immersing in solutions with increasing concentrations of ethanol (25%, 50%, 75%, 95%, and 100%) for 10 min each. After platinum coating for 40 s, all samples were analyzed by FE-SEM. Relative bacterial adhesion onto PPE fabrics according to the molar ratio of poly(DMA-PEGMA-QA) was quantified using crystal violet (CV) assays. PPE fabrics incubated with *S. aureus* were stained with 0.1% CV solution (Becton, Dickinson and Company, Franklin Lakes, NJ, USA) for 15 min, after which excess CV dye was removed by washing twice with 1 \times PBS, followed by extraction of stained CV dye using a decolorizer (Becton, Dickinson and Company) and measurement of OD_{580} .

Antibacterial Effect of Poly(DMA-PEGMA-QA)-Coated PPE Fabrics. The membrane distortion of bacteria after incubating the polymer-coated PPE surface with *S. aureus* for 24 h in a 37 °C incubator was assessed in PPE samples fixed with 4% formaldehyde and serially dehydrated using increasing concentrations of ethanol. The samples were observed by FE-SEM at 25 000 \times magnification. After incubation, remaining viable bacteria were quantified by detaching bacteria from all PPE samples using a consistent vortexing pulse and sonication. The relative number of detached viable bacteria was quantified using WST-8 reagent (Roche, Mannheim, Germany). After incubation with WST-8 reagent (diluted 1:10 with PBS) for 2 h, the optical density of the solution was measured at 440 nm and the reference intensity was determined at 690 nm. Live bacteria on PPE surfaces after incubation were further

quantified by counting CFUs on blood agar plates (Komed, Seongnam, Korea). Briefly, bacteria detached from PPE fabrics were serially diluted 100-, 1000-, and 10 000-fold, spread onto blood agar plates, and incubated for 16 h at 37 °C, after which CFUs were counted.

To evaluate the antibacterial ability of polymer-coated PPE in an airborne condition, *S. aureus* cultured in LB media was first washed with sterile 0.85% NaCl solution. The resulting bacterial suspension was concentrated via centrifuge at 10 000 rpm for 10 min and prepared in 0.85% NaCl solution at $\sim 5 \times 10^8$ CFU/mL. Subsequently, a bacterial suspension was sprayed onto each PPE fabric for 3 s using a chromatography sprayer connected to an air gun. After even spraying of the bacterial solution onto PPE fabrics, all fabric samples were incubated at room temperature for 0.5, 1, and 2 h. After the indicated period, the bacterial-sprayed fabrics were gently vortexed and sonicated while immersed in 0.85% NaCl solution. The viability of the bacteria in the collected solutions was assessed by the L/D bacterial viability kit. To quantify the viability of the bacterial suspension, we generated a standard curve using a live and dead bacterial mixture where the dead bacteria for the standard curve was prepared by incubating in 70% ethanol for 20 min.

Antiviral Effects of Poly(DMA-mPEGMA-QA) and Coated PPE Fabrics. Vero-E6 cells were cultured in Dulbecco's Minimal Essential Medium (DMEM; Welgene, Gyeongsan, Korea) supplemented with 10% fetal bovine serum (FBS; Welgene) and 1% antibiotic antimycotic solution (ThermoFisher Scientific, Waltham, MA, USA). PEDV was inoculated into Vero-E6 cultures (in DMEM) supplemented with 0.3% tryptose phosphate broth, 0.02% yeast extract, and 2 μ g of trypsin. Viral titers were determined as the $TCID_{50}$ on Vero-E6 cells and expressed as the reciprocal of the highest virus dilution showing a cytopathic effect in a 96-well plate. PEDV titration was performed using 96-well plates containing Vero-E6 cells seeded at 2×10^4 cells/well. After washing confluent cells in the microplate three times with PBS, five wells were inoculated with 0.1 mL per well of a 10-fold serially diluted PEDV suspension. Following stabilization for 1 h at 37 °C, inocula were removed, and the cells were washed once with PBS. Thereafter, 0.2 mL of fresh virus replication medium supplemented with 0.3% tryptose phosphate broth, 0.02% yeast extract, and 2 μ g of trypsin were transferred into each well, and the cells were further incubated for 5 days at 37 °C. The antiviral effect of poly(DMA-PEGMA-QA) against coronavirus was evaluated by mixing 20 mg/mL polymer synthesized at different molar ratios with a PEDV suspension at a 1:1 (v/v) ratio for 1 h at 4 °C. After incubation, the mixture was centrifuged at 10 000 rpm for 10 min at 4 °C, and the titer of the supernatant was assessed using $TCID_{50}$ assays. In concurrent assays, PPE surfaces spray-coated with 20 mg/mL poly(DMA-PEGMA-QA) at four different molar feed ratios were treated with 0.5 mL of the coronavirus and incubated for 1 h at 4 °C. The incubated virus was collected and quantified using $TCID_{50}$ assays. The viability of the remaining viruses in the PPE fabric was also analyzed by collecting PPE samples with the virus, vortexing with 1 mL of the growth medium, and performing $TCID_{50}$ assays on the supernatant.

Biocompatibility of Poly(DMA-PEGMA-QA) Coating. The mouse fibroblast cell line NIH-3T3 (ATCC CRL-1658) was used for *in vitro* cytotoxicity assays of poly(DMA-mPEGMA-QA). Briefly, a 96-well plate was coated with

polymer at two molar ratios that showed the best antiviral efficacy (3.5:6:0.5 and 3.5:5.5:1). NIH-3T3 cells were seeded on a polymer-coated, 96-well culture plate and cultured for 24 h at 37 °C in a humidified 5% CO₂ atmosphere. Following incubation, the viability of cultured cells was assessed using the WST-8 reagent. For *in vivo* biocompatibility tests, PPE fabric was spray-coated with poly(DMA-PEGMA-QA) at the highest concentration that showed no *in vitro* cytotoxicity (100 mg/mL) and that could be used at a working concentration of 20 mg/mL. Polymer coated-PPE fabrics were attached to the shaved backs of 7 week-old, male C57BL/6 mice (OrientBio, Seongnam, Korea). After 24 h of skin contact, the mice were euthanized and the skin in contact with the polymer-coated PPE was collected. Inflammation and irritation in collected skins were analyzed by Draize scoring, H&E staining, and TB staining. All animal studies were performed with approval of the Institutional Animal Care and Use Committee (IACUC) of the Korea Advanced Institute of Science and Technology (KAIST) (Accreditation number: KA2020-47).

■ ASSOCIATED CONTENT

SI Supporting Information

The Supporting Information is available free of charge at <https://pubs.acs.org/doi/10.1021/acsomega.1c04919>.

Representative ¹H NMR spectrum of poly(DMA-PEGMA-DMAEMA) (Figure S1); ¹H NMR spectra of poly(DMA-PEGMA-QA) (Figure S2); MALDI-TOF measurements of poly(DMA-PEGMA-QA) prepared from different molar ratios of each monomer (Figure S3); surface roughness of poly(DMA-PEGMA-QA)-coated PPE fabric (Figure S4); the coating stability analyzed by water contact angle measurements (Figure S5); the comparison of the antimicrobial effect of poly(DMA-PEGMA-AA) and poly(DMA-PEGMA-QA)-coated PPE fabric (Figure S6); the long-term antimicrobial effect of poly(DMA-PEGMA-QA)-coated PPE fabric (Figure S7); evaluation of local inflammation caused by polymer-coated PPE assessed by quantification of infiltrated mast cells (Figure S8); evaluation of systemic inflammation caused by polymer-coated PPE (Figure S9) (PDF)

■ AUTHOR INFORMATION

Corresponding Author

Sangyong Jon – KAIST Institute for the BioCentury,
Department of Biological Sciences and Center for Precision
Bio-Nanomedicine, Korea Advanced Institute of Science and
Technology (KAIST), Daejeon 34141, Republic of Korea;
✉ orcid.org/0000-0002-6971-586X; Email: syjon@kaist.ac.kr

Authors

Hyeongseop Keum – KAIST Institute for the BioCentury,
Department of Biological Sciences and Center for Precision
Bio-Nanomedicine, Korea Advanced Institute of Science and
Technology (KAIST), Daejeon 34141, Republic of Korea
Dohyeon Kim – KAIST Institute for the BioCentury,
Department of Biological Sciences and Center for Precision
Bio-Nanomedicine, Korea Advanced Institute of Science and
Technology (KAIST), Daejeon 34141, Republic of Korea;
✉ orcid.org/0000-0002-0978-6885

Chang-Hee Whang – KAIST Institute for the BioCentury,
Department of Biological Sciences and Center for Precision
Bio-Nanomedicine, Korea Advanced Institute of Science and
Technology (KAIST), Daejeon 34141, Republic of Korea
Aram Kang – College of Pharmacy, Korea University, Sejong
30019, Republic of Korea

Seojung Lee – KAIST Institute for the BioCentury,
Department of Biological Sciences and Center for Precision
Bio-Nanomedicine, Korea Advanced Institute of Science and
Technology (KAIST), Daejeon 34141, Republic of Korea;
✉ orcid.org/0000-0002-7835-3450

Woonsung Na – College of Veterinary Medicine, Chonnam
University, Gwangju 61186, Republic of Korea

Complete contact information is available at:

<https://pubs.acs.org/doi/10.1021/acsomega.1c04919>

Author Contributions

†H.K. and D.K. contributed equally to this work. S.J. conceived the project, and S.J., H.K., and D.K. wrote the paper. H.K. performed most of the experiments, and S.J., H.K., and W.N. analyzed the data. D.K., C.-H.W., A.K., and S.L. carried out certain experiments. All authors have approved the final version of the manuscript.

Notes

The authors declare no competing financial interest.

■ ACKNOWLEDGMENTS

This research was supported by the Basic Science Research Program (Leading Researcher Program: NRF-2018R1A3B1052661), Global Ph.D. Fellowship Program (NRF-2019H1A2A1074396), and KAIST Mobile Clinic Module Project (MCM-2020-N11200214) funded by the Ministry of Science and ICT. The illustrations were created with [BioRender.com](https://www.bio-render.com).

■ REFERENCES

- (1) Cohen, J.; Rodgers, Y. V. Contributing factors to personal protective equipment shortages during the COVID-19 pandemic. *Prev Med.* **2020**, *141*, 106263.
- (2) Riddell, S.; Goldie, S.; Hill, A.; Eagles, D.; Drew, T. W. The effect of temperature on persistence of SARS-CoV-2 on common surfaces. *Virology* **2020**, *17* (1), 145.
- (3) Chia, P. Y.; Coleman, K. K.; Tan, Y. K.; Ong, S. W. X.; Gum, M.; Lau, S. K.; Lim, X. F.; Lim, A. S.; Sutjipto, S.; Lee, P. H.; Son, T. T.; Young, B. E.; Milton, D. K.; Gray, G. C.; Schuster, S.; Barkham, T.; De, P. P.; Vasoo, S.; Chan, M.; Ang, B. S. P.; Tan, B. H.; Leo, Y.-S.; Ng, O.-T.; Wong, M. S. Y.; Marimuthu, K. Detection of air and surface contamination by SARS-CoV-2 in hospital rooms of infected patients. *Nat. Commun.* **2020**, *11* (1), 2800.
- (4) Dowell, S. F.; Simmerman, J. M.; Erdman, D. D.; Wu, J. S. J.; Chaovanich, A.; Javadi, M.; Yang, J. Y.; Anderson, L. J.; Tong, S. X.; Ho, M. S. Severe acute respiratory syndrome coronavirus on hospital surfaces. *Clin Infect Dis* **2004**, *39* (5), 652–657.
- (5) Song, J. J.; Noh, I.; Chae, S. W. Inhibition of Biofilm Formation on Ventilation Tubes by Surface Modification. *In Vivo* **2012**, *26* (6), 907–911.
- (6) Liu, Z. Y.; Jiang, Q.; Jin, Z. Q.; Sun, Z. Y.; Ma, W. J.; Wang, Y. L. Understanding the Antifouling Mechanism of Zwitterionic Monomer-Grafted Polyvinylidene Difluoride Membranes: A Comparative Experimental and Molecular Dynamics Simulation Study. *ACS Appl. Mater. Inter* **2019**, *11* (15), 14408–14417.
- (7) He, M. R.; Gao, K.; Zhou, L. J.; Jiao, Z. W.; Wu, M. Y.; Cao, J. L.; You, X. D.; Cai, Z. Y.; Su, Y. L.; Jiang, Z. Y. Zwitterionic materials for antifouling membrane surface construction. *Acta Biomater* **2016**, *40*, 142–152.

- (8) Wei, T.; Tang, Z.; Yu, Q.; Chen, H. Smart Antibacterial Surfaces with Switchable Bacteria-Killing and Bacteria-Releasing Capabilities. *ACS Appl. Mater. Interfaces* **2017**, *9* (43), 37511–37523.
- (9) Shi, H. C.; Liu, H. Y.; Luan, S. F.; Shi, D.; Yan, S. J.; Liu, C. M.; Li, R. K. Y.; Yin, J. H. Effect of polyethylene glycol on the antibacterial properties of polyurethane/carbon nanotube electrospun nanofibers. *Rsc Adv.* **2016**, *6* (23), 19238–19244.
- (10) Jeong, G. M.; Seong, H.; Im, S. G.; Sung, B. H.; Kim, S. C.; Jeong, K. J. Coating of an antimicrobial peptide on solid substrate via initiated chemical vapor deposition. *J. Ind. Eng. Chem.* **2018**, *58*, 51–56.
- (11) He, J. C.; Chen, J. J.; Hu, G. S.; Wang, L.; Zheng, J.; Zhan, J. Z.; Zhu, Y. C.; Zhong, C. T.; Shi, X. T.; Liu, S.; Wang, Y. J.; Ren, L. Immobilization of an antimicrobial peptide on silicon surface with stable activity by click chemistry. *J. Mater. Chem. B* **2018**, *6* (1), 68–74.
- (12) Bu, Y. M.; Zhang, S. Y.; Cai, Y. J.; Yang, Y. Y.; Ma, S. T.; Huang, J. J.; Yang, H. J.; Ye, D. Z.; Zhou, Y. S.; Xu, W. L.; Gu, S. J. Fabrication of durable antibacterial and superhydrophobic textiles via in situ synthesis of silver nanoparticle on tannic acid-coated viscose textiles. *Cellulose* **2019**, *26* (3), 2109–2122.
- (13) Li, X.; Huang, T.; Heath, D. E.; O'Brien-Simpson, N. M.; O'Connor, A. J. Antimicrobial nanoparticle coatings for medical implants: Design challenges and prospects. *Biointerphases* **2020**, *15* (6), 060801.
- (14) Wang, Y. D.; Yuan, X.; Li, H.; Liu, L. J.; Zhao, F. B.; Wang, G.; Wang, Q.; Yu, Q. Antibacterial and drug-release dual-function membranes of cross-linked hyperbranched cationic polymers. *React. Funct. Polym.* **2020**, *157*, 104749.
- (15) Pan, Y. F.; Xia, Q. Y.; Xiao, H. N. Cationic Polymers with Tailored Structures for Rendering Polysaccharide-Based Materials Antimicrobial: An Overview. *Polymers-Basel* **2019**, *11* (8), 1283.
- (16) Cox, G.; Wright, G. D. Intrinsic antibiotic resistance: Mechanisms, origins, challenges and solutions. *Int. J. Med. Microbiol.* **2013**, *303* (6–7), 287–292.
- (17) Silhavy, T. J.; Kahne, D.; Walker, S. The Bacterial Cell Envelope. *Cold Spring Harbor Perspect. Biol.* **2010**, *2* (5), a000414.
- (18) Qiu, H. F.; Si, Z. Y.; Luo, Y.; Feng, P. P.; Wu, X. J.; Hou, W. J.; Zhu, Y. B.; Chan-Park, M. B.; Xu, L.; Huang, D. M. The Mechanisms and the Applications of Antibacterial Polymers in Surface Modification on Medical Devices. *Front Bioeng Biotech* **2020**, *8*, 1.
- (19) Dong, J. J.; Muszanska, A.; Xiang, F.; Falkenberg, R.; van de Belt-Gritter, B.; Loontjens, T. Contact Killing of Gram-Positive and Gram-Negative Bacteria on PDMS Provided with Immobilized Hyperbranched Antibacterial Coatings. *Langmuir* **2019**, *35* (43), 14108–14116.
- (20) Keum, H.; Kim, J. Y.; Yu, B.; Yu, S. J.; Kim, J.; Jeon, H.; Lee, D. Y.; Im, S. G.; Jon, S. Prevention of Bacterial Colonization on Catheters by a One-Step Coating Process Involving an Antibiofouling Polymer in Water. *ACS Appl. Mater. Inter* **2017**, *9* (23), 19736–19745.
- (21) Xue, Y.; Xiao, H.; Zhang, Y. Antimicrobial polymeric materials with quaternary ammonium and phosphonium salts. *Int. J. Mol. Sci.* **2015**, *16* (2), 3626–55.
- (22) Fuchs, A. D.; Tiller, J. C. Contact-active antimicrobial coatings derived from aqueous suspensions. *Angew. Chem., Int. Ed. Engl.* **2006**, *45* (40), 6759–62.
- (23) Zheng, A. N.; Xu, X.; Xiao, H. N.; Guan, Y.; Li, S. Z.; Wei, D. F. Preparation of antistatic and antimicrobial polyethylene by incorporating of comb-like ionenes. *J. Mater. Sci.* **2012**, *47* (20), 7201–7209.
- (24) Zainul Abid, C. K. V.; Jackeray, R.; Jain, S.; Chattopadhyay, S.; Asif, S.; Singh, H. Antimicrobial Efficacy of Synthesized Quaternary Ammonium Polyamidoamine Dendrimers and Dendritic Polymer Network. *J. Nanosci. Nanotechnol.* **2016**, *16* (1), 998–1007.
- (25) Abid, C. K. V. Z.; Chattopadhyay, S.; Mazumdar, N.; Singh, H. Synthesis and Characterization of Quaternary Ammonium PEGDA Dendritic Copolymer Networks for Water Disinfection. *J. Appl. Polym. Sci.* **2010**, *116* (3), 1640–1649.
- (26) Eren, T.; Som, A.; Rennie, J. R.; Nelson, C. F.; Urgina, Y.; Nusslein, K.; Coughlin, E. B.; Tew, G. N. Antibacterial and hemolytic activities of quaternary pyridinium functionalized polynorbornenes. *Macromol. Chem. Phys.* **2008**, *209* (5), 516–524.
- (27) Gerba, C. P. Quaternary Ammonium Biocides: Efficacy in Application. *Appl. Environ. Microb.* **2015**, *81* (2), 464–469.
- (28) Daood, U.; Matinlinna, J. P.; Pichika, M. R.; Mak, K. K.; Nagendrababu, V.; Fawzy, A. S. A quaternary ammonium silane antimicrobial triggers bacterial membrane and biofilm destruction. *Sci. Rep.-Uk* **2020**, *10* (1), 10970.
- (29) Jennings, M. C.; Minbiole, K. P. C.; Wuest, W. M. Quaternary Ammonium Compounds: An Antimicrobial Mainstay and Platform for Innovation to Address Bacterial Resistance. *ACS Infect Dis* **2015**, *1* (7), 288–303.
- (30) Damodaran, V. B.; Murthy, N. S. Bio-inspired strategies for designing antifouling biomaterials. *Biomater Res.* **2016**, *20*, 18.
- (31) Xie, Q.; Pan, J.; Ma, C.; Zhang, G. Dynamic surface antifouling: mechanism and systems. *Soft Matter* **2019**, *15* (6), 1087–1107.
- (32) Ten Broek, R. P.; Kok-Krant, N.; Verhoeve, H. R.; van Goor, H.; Bakkum, E. A. Efficacy of polyethylene glycol adhesion barrier after gynecological laparoscopic surgery: Results of a randomized controlled pilot study. *Gynecol Surg* **2012**, *9* (1), 29–35.
- (33) Jennings, M. C.; Buttaro, B. A.; Minbiole, K. P. C.; Wuest, W. M. Bioorganic Investigation of Multicationic Antimicrobials to Combat QAC-Resistant *Staphylococcus aureus*. *ACS Infect Dis* **2015**, *1* (7), 304–309.
- (34) Tuladhar, E.; Hazeleger, W. C.; Koopmans, M.; Zwietering, M. H.; Beumer, R. R.; Duizer, E. Residual Viral and Bacterial Contamination of Surfaces after Cleaning and Disinfection. *Appl. Environ. Microb.* **2012**, *78* (21), 7769–7775.
- (35) Yamanaka, T.; Bannai, H.; Tsujimura, K.; Nemoto, M.; Kondo, T.; Matsumura, T. Comparison of the Virucidal Effects of Disinfectant Agents Against Equine Influenza A Virus. *J. Equine Vet Sci.* **2014**, *34* (5), 715–718.
- (36) Ding, Y.; Klyushin, A.; Huang, X.; Jones, T.; Teschner, D.; Girgsdies, F.; Rodenas, T.; Schlogl, R.; Heumann, S. Cobalt-Bridged Ionic Liquid Polymer on a Carbon Nanotube for Enhanced Oxygen Evolution Reaction Activity. *Angew. Chem., Int. Ed. Engl.* **2018**, *57* (13), 3514–3518.
- (37) Plank, U.; Meisl, G.; von Toussaint, U.; Hoschen, T.; Jacob, W. Study of the temperature-dependent nitrogen retention in tungsten surfaces using X-ray photoelectron spectroscopy. *Nucl. Mater. Energy* **2018**, *17*, 48–55.
- (38) Siu, J. H. W.; Li, L. K. Y. An investigation of the effect of surface roughness and coating thickness on the friction and wear behaviour of a commercial MoS₂-metal coating on AISI 400C steel. *Wear* **2000**, *237* (2), 283–287.
- (39) Lacombe, A.; Gomes-Fernandes, M.; Mesalles, E.; Armestar, F.; Villar, R.; Casas, I.; Molinos, S.; Gimenez, M.; Ausina, V.; Prat, C. Persistence of *Staphylococcus aureus* in lower respiratory tract in patients undergoing mechanical ventilation. *Eur. Respir. J.* **2015**, *46*, PA2640.
- (40) Parker, D.; Prince, A. Immunopathogenesis of *Staphylococcus aureus* pulmonary infection. *Semin Immunopathol* **2012**, *34* (2), 281–297.
- (41) Tilahun, B.; Faust, A. C.; McCorstin, P.; Ortegón, A. Nasal Colonization and Lower Respiratory Tract Infections with Methicillin-Resistant *Staphylococcus aureus*. *Am. J. Crit Care* **2015**, *24* (1), 8–12.
- (42) Bouloussa, H.; Saleh-Mghir, A.; Valotteau, C.; Cherifi, C.; Hafsia, N.; Cohen-Solal, M.; Court, C.; Cremieux, A. C.; Humblot, V. A Graftable Quaternary Ammonium Biocidal Polymer Reduces Biofilm Formation and Ensures Biocompatibility of Medical Devices. *Adv. Mater. Interfaces* **2021**, *8* (5), 2001516.
- (43) Kim, S.; Girn, T.; Jeong, Y.; Ryu, J. H.; Kang, S. M. Facile Construction of Robust Multilayered PEG Films on Polydopamine-Coated Solid Substrates for Marine Antifouling Applications. *ACS Appl. Mater. Inter* **2018**, *10* (9), 7626–7631.
- (44) Lowe, S.; O'Brien-Simpson, N. M.; Connal, L. A. Antibiofouling polymer interfaces: poly(ethylene glycol) and other promising candidates. *Polym. Chem-Uk* **2015**, *6* (2), 198–212.

- (45) Farah, S.; Aviv, O.; Laout, N.; Ratner, S.; Beyth, N.; Domb, A. J. Quaternary ammonium poly(diethylaminoethyl methacrylate) possessing antimicrobial activity. *Colloid Surface B* **2015**, *128*, 608–613.
- (46) Shen, Z.; Ye, G.; Deng, F.; Wang, G.; Cui, M.; Fang, L.; Xiao, S.; Fu, Z. F.; Peng, G. Structural Basis for the Inhibition of Host Gene Expression by Porcine Epidemic Diarrhea Virus nsp1. *J. Virol* **2018**, *92* (5), 1.
- (47) Kirchdoerfer, R. N.; Bhandari, M.; Martini, O.; Sewall, L. M.; Bangaru, S.; Yoon, K. J.; Ward, A. B. Structure and immune recognition of the porcine epidemic diarrhea virus spike protein. *Structure* **2021**, *29* (4), 385–392.
- (48) Simula, E. R.; Manca, M. A.; Jasemi, S.; Uzzau, S.; Rubino, S.; Manchia, P.; Bitti, A.; Palermo, M.; Sechi, L. A. HCoV-NL63 and SARS-CoV-2 Share Recognized Epitopes by the Humoral Response in Sera of People Collected Pre- and during CoV-2 Pandemic. *Microorganisms* **2020**, *8* (12), 1993.
- (49) Sung, D.; Park, S.; Jon, S. Facile Method for Selective Immobilization of Biomolecules on Plastic Surfaces. *Langmuir* **2009**, *25* (19), 11289–11294.
- (50) Draelos, Z.; Hornby, S.; Walters, R. M.; Appa, Y. Hydrophobically modified polymers can minimize skin irritation potential caused by surfactant-based cleansers. *J. Cosmet Dermatol-Us* **2013**, *12* (4), 314–321.
- (51) Panda, S. K.; Facchinetti, V.; Voynova, E.; Hanabuchi, S.; Karnell, J. L.; Hanna, R. N.; Kolbeck, R.; Sanjuan, M. A.; Ettinger, R.; Liu, Y. J. Galectin-9 inhibits TLR7-mediated autoimmunity in murine lupus models. *J. Clin Invest* **2018**, *128* (5), 1873–1887.
- (52) Jawhar, M.; Schwaab, J.; Hausmann, D.; Clemens, J.; Naumann, N.; Henzler, T.; Horny, H. P.; Sotlar, K.; Schoenberg, S. O.; Cross, N. C.; Fabarius, A.; Hofmann, W. K.; Valent, P.; Metzgeroth, G.; Reiter, A. Splenomegaly, elevated alkaline phosphatase and mutations in the SRSF2/ASXL1/RUNX1 gene panel are strong adverse prognostic markers in patients with systemic mastocytosis. *Leukemia* **2016**, *30* (12), 2342–2350.